

Article

An Analytical Solution of Transient Wave Generation in the Wave Channel

Cheng-Tsung Chen ¹, Jaw-Fang Lee ^{2,3,*} , Kuei-Ting Lin ⁴ and Pi-Sheng Hu ⁵

¹ School of Information Engineering, Sanming University, Sanming 365004, China

² Tainan Hydraulics Laboratory, National Cheng Kung University, Tainan 70101, Taiwan

³ Center for Innovative Research on Aging Society, National Chung Cheng University, Chiayi 621301, Taiwan

⁴ Construction and Tourism Section, Lukan Township Office, Changhua 505006, Taiwan

⁵ Science Education Center, National Cheng Kung University, Tainan 70101, Taiwan

* Correspondence: jflee@mail.ncku.edu.tw

Abstract: Transient characteristics of wave generation in the wave channel can provide unique and important information in contrast to the steady and periodic motion of propagation waves. In this paper, a new analytical solution is proposed for a transient wavemaker problem in the wave channel. The mathematical model of the wavemaker problem is established based on the linear potential wave theory, and a new analytical solution for the corresponding initial and boundary-value problem is presented. The present solution methodology is motivated and developed from old methods shown in literature. The present solution can be mathematically reformulated and shown to be identical to the previous solution using different solution methodology. The present analytical solution is further compared with numerical results and experiments to validate the mathematical model. The present solution is used to calculate the steady state generated wave forms that compare very well with the steady wave theory both in wave length and wave period. The present solution is also used to study unsteady characteristics of wave heights and wave lengths of the leading waves. The present analytical solution methodology can provide an easier approach to obtain the analytical solution for transient wave generation problem in the wave channel.



Citation: Chen, C.-T.; Lee, J.-F.; Lin, K.-T.; Hu, P.-S. An Analytical Solution of Transient Wave Generation in the Wave Channel. *J. Mar. Sci. Eng.* **2022**, *10*, 1198. <https://doi.org/10.3390/jmse10091198>

Academic Editor: Alon Gany

Received: 25 July 2022

Accepted: 24 August 2022

Published: 26 August 2022

Publisher's Note: MDPI stays neutral with regard to jurisdictional claims in published maps and institutional affiliations.



Copyright: © 2022 by the authors. Licensee MDPI, Basel, Switzerland. This article is an open access article distributed under the terms and conditions of the Creative Commons Attribution (CC BY) license (<https://creativecommons.org/licenses/by/4.0/>).

Keywords: transient; wavemaker; wave channel; analytical solution

1. Introduction

Wave generations in the laboratory, either wave channels or plane basins, are important related to performing experiments in studying wave characteristics or wave and structure interactions. Recent literature related to various types of wave generations, i.e., plunger or wedge type wavemakers, or wave characteristics regarding deep or intermediate waters, can be found in [1–3]. Wavemaker theories are associated with wave generations; however, they are mostly steady and periodic solutions as far as analytical solutions are concerned. Transient wave generations concentrate on the entire wave development or decaying processes, but analytical solutions due to the inherited mathematical complexities are not so much available [4]. For fully nonlinear water wave problems, inevitably, numerical methods are eventually good approaches to solve the problems. Jang and Sung [5] used the smoothed particle hydrodynamics (SPH) method to simulate the piston-type wavemaker problem. In the numerical scheme, the fluid phase was discretized into a distribution of small fluid particles, whose dynamics were influenced by neighboring particles that lay within a support domain. For a given particle, the effect of the surrounding fluid was determined by a weighted sum over all the remaining particles in the system. Wei and Kirby [6] on the other hand used an extended Boussinesq equation to govern the water wave motions, and a numerical code was given to simulate the time-dependent problems. De Padova et al. [7] utilized the SPH numerical method to simulate the wave domain, while the buoyant jet was coexisting in the fluid domain. The characteristics of the buoyant jets affecting by the

wave motion were investigated. Ozbulut et al. [8] utilized the Navier–Stokes and continuity equations for governing the fluid motion through the Weakly Compressible SPH (WCSPH) approach to simulate wave generations in the wave tank. Gholamipour and Ghiasi [9] developed a numerical wave tank (NWT) by employing the local radial point interpolation collocation method, mixed Eulerian–Lagrangian approach, and the fourth order Runge–Kutta method. The potential theory was used for the mathematical description of the wave propagation problem. Vivanco et al. [10] used the SPH simulation and introduced a framework for wave generation through the action of the pedal-wavemaking method, which generates long waves without effects of evanescent waves. The other category was the wide use of the open-source OpenFOAM CFD libraries, together with methods that were commonly used to deal with wave generation and absorption [11–13].

For analytical solutions to unsteady wave generation problems, Lee et al. [14] proposed a transient wavemaker theory. The time function was resolved by using the Laplace transform, the x function was expressed by the Fourier cosine function, and the z function was obtained by a direct integration method. The solution could be obtained without any difficulty, but the inversed Laplace transform was complicated and could involve numerical calculations for some mathematical functions. Reviews of some hydrodynamic characteristics of transient waves were given in references therein. Lee [15] used the same solution methodology to solve for a piston-type wavemaker problem. Comparisons of unsteady wave characteristics generated by flap-type and piston-type wavemaker were discussed. Joo et al. [16] also proposed an analytical solution to the initial and boundary-value problem of the wavemaker problems. A boundary condition on the wavemaker was presented. The unique part of the solution was a particular solution satisfying the time-dependent wavemaker boundary condition. Chang et al. [17] solved the piston-type wavemaker problem using a similar solution approach, and Lin et al. [18] solved the wavemaker problems generating irregular waves. Note that in this approach it was necessary to have a particular solution to satisfy the boundary condition that was in some cases difficult to derive.

The phenomena of undular bores at water surface also have transient characteristics while propagating along the water channel. The associated analytical solutions could possibly be applied for the transient wavemaker problems. Berry [19] applied the quantum and Hawking effect analogies to describe analytically a model for undular bore profile. EI et al. [20] presented an asymptotic analytical description for undular bores, in which the Whitham modulation theory and the Su–Gardner system were used together with the Boussinesq governing equation. Landrini and Tyvand [21] analytically and numerically studied the free surface flow induced by impulsive bottom movements. Marchant [22] adopted the modified Korteweg–de Vries equation and presented analytical solutions for undular bores. Bestehorn and Tyvand [23] solved nonlinear, two-dimensional Laplace equation and studied interactions between two undular bores in a long rectangular channel. Ali and Kalisch [24] studied the dispersive undular bore model and concluded that there was no energy loss in the dispersive model. Chen et al. [25] presented a mathematical model to simulate undular bores generated by blocking steady water currents in a flume, and an analytical solution was presented. Tong and Liu [26] presented an analytical solution for studying transient water wave-induced responses inside an unsaturated poroelastic seabed of finite thickness. The transient waves, including the linear periodic wave, a solitary wave, and a bore, were considered.

In this study, a new analytical solution for the transient wavemaker problems in a wave channel is presented. The proposed method follows Chen et al. [25], which combined the applicability approach of Lee et al. [14] and Joo et al. [16]. Our analytical solution is applied to simulate wave evolutions generated by the wavemaker motions. The generated steady state wave forms are compared with the steady state analytical solution given by Dean and Dalrymple [27], and characteristics of evanescent waves are identified. Finally, we demonstrate capabilities of the present analytical solution by showing the generated wave forms along the wave channel at an integer number of periods of the wavemaker

motion, and transient characteristics of wave generation regarding leading wave lengths and wave heights are investigated.

2. Problem Description and Solution

The problem of wave generation by a wavemaker in a wave channel was sketched, as shown in Figure 1. The length of the channel was ℓ , the constant water depth was h . A piston type wavemaker was specified at the left-hand side, and the end of the channel was a vertical wall. With an initially still water surface, and given that the wavemaker started with periodic motion, it was expected to have wave motions in front of the wavemaker, which also propagate toward the end of the channel. A Cartesian coordinate system with the origin located at the still water level was chosen, as indicated in Figure 1. The positive x axis pointed to the right and the positive z axis pointed upward.

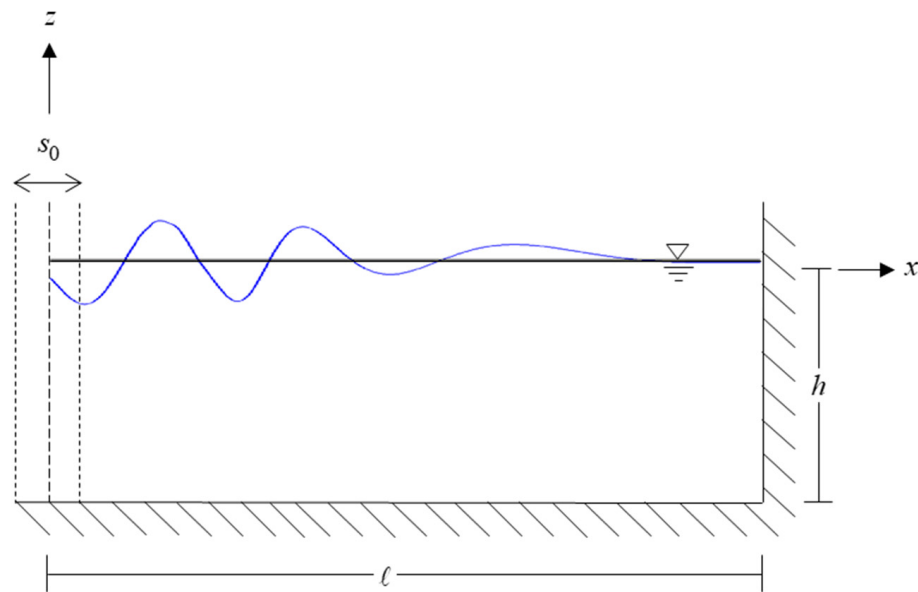


Figure 1. Definition sketch of the wavemaker problem in a channel.

In this study, the wave motions in the channel are described by using the linear potential wave theory. The relation of the flow velocity V and the potential function Φ is given by

$$\vec{V}(x, z, t) = -\nabla\Phi(x, z, t) \tag{1}$$

where ∇ is the Laplacian operator. The boundary-value problem can be expressed as [27].

The governing equation is the Laplace equation:

$$\nabla^2\Phi(x, z, t) = 0 \tag{2}$$

The free surface boundary condition and the bottom condition can be written, respectively, as

$$\frac{\partial\Phi}{\partial z} + \frac{1}{g} \frac{\partial^2\Phi}{\partial t^2} = 0, \quad z = 0 \tag{3}$$

$$\frac{\partial\Phi}{\partial z} = 0, \quad z = -h \tag{4}$$

where g is the gravity constant. The wavemaker boundary condition at $x = 0$ is

$$\frac{\partial\Phi}{\partial x} = -\dot{\zeta}(t), \quad x = 0 \tag{5}$$

where $\zeta(t)$ is the displacement function of the wavemaker and the upper dot indicates time derivative. At the right-hand end vertical wall, the boundary condition is

$$\frac{\partial \Phi}{\partial x} = 0, \quad x = \ell \tag{6}$$

The initial conditions considered in this paper were the still water in the channel and no disturbances at the free surface. Equations (2)–(6), together with the initial conditions, represent the initial and boundary-value problem shown in Figure 1. In the following, an analytical solution to the problem will be described.

The potential function $\Phi(x, z, t)$ was a function of spatial coordinates (x, z) and time t . The first step of the present solution was to solve the x function. Equations (2)–(6) were reformulated using the Fourier cosine transform. The x function was expressed in terms of the finite Fourier cosine series, and the potential function could be expressed as [28]

$$\Phi(x, z, t) = \frac{1}{\ell} \phi_0(z, t) + \frac{2}{\ell} \sum_{n=1} \phi_n(z, t) \cos(\omega_n x) \tag{7}$$

where $\omega_n = n\pi/\ell$ and ϕ_0, ϕ_n are defined, respectively, as

$$\phi_0(z, t) = \int_0^\ell \Phi(x, z, t) dx \tag{8}$$

$$\phi_n(z, t) = \int_0^\ell \Phi(x, z, t) \cdot \cos(\omega_n x) dx \tag{9}$$

The use of the cosine functions can facilitate implements of boundary conditions at two ends of the channel, as can be observed later in the solution formulation.

The solution step then turned to solve the z function included in $\phi_0(z, t)$ and $\phi_n(z, t)$. In the following, only the solution of $\phi_n(z, t)$ is given, as the solution to $\phi_0(z, t)$ is only a special case of $\phi_n(z, t)$. The governing equation, the free surface, and bottom conditions, Equations (2)–(4), were rewritten, following the Fourier cosine transform of Equation (9), as

$$\frac{\partial^2 \phi_n(z, t)}{\partial z^2} - \omega_n^2 \phi_n(z, t) = -\dot{\zeta}(t) \tag{10}$$

$$\frac{\partial \phi_n}{\partial z} + \frac{1}{g} \frac{\partial^2 \phi_n}{\partial t^2} = 0, \quad z = 0 \tag{11}$$

$$\frac{\partial \phi_n}{\partial z} = 0, \quad z = -h \tag{12}$$

Equation (10) was a non-homogeneous second-order differential equation, and the solution can be obtained by using the method of variation of parameters [28] and written as [28]

$$\phi_n(z, t) = \tilde{\phi}_{nh}(z, t) + \tilde{\phi}_{np}(z, t) \tag{13}$$

in which $\tilde{\phi}_{nh}$ and $\tilde{\phi}_{np}$ are the homogeneous solution and the particular solution, respectively. The solution to Equation (13) was

$$\tilde{\phi}_{nh}(z, t) = A_n(t)e^{\omega_n z} + B_n(t)e^{-\omega_n z} \tag{14}$$

$$\tilde{\phi}_{np}(z, t) = \frac{\dot{\zeta}}{\omega_n^2} \tag{15}$$

where $A_n(t)$ and $B_n(t)$ could be determined by utilizing the free surface and bottom boundary conditions, Equations (11) and (12).

The substitutions of Equations (13)–(15) into the free surface and bottom boundary conditions yield

$$\ddot{B}_n(t) + k_n^2 B_n(t) = \frac{-\ddot{\xi}}{\omega_n^2(e^{2\omega_n h} + 1)} \tag{16}$$

$$A_n(t) = B_n(t)e^{2\omega_n h} \tag{17}$$

where $k_n = \sqrt{g\omega_n \tanh(\omega_n h)}$. Equation (16) is a second-order differential equation in time solving for B_n , and Equation (17) is a relation between the coefficients A_n and B_n . The solution of Equation 16 can be written as

$$B_n(t) = D_n \cdot e^{ik_n t} + E_n \cdot e^{-ik_n t} + B_n^p(t) \tag{18}$$

where D_n and E_n are the integration constants, whereas

$$B_n^p(t) = \frac{i \left[\left(\int \ddot{\xi} e^{-ik_n t} dt \right) e^{ik_n t} - \left(\int \ddot{\xi} e^{ik_n t} dt \right) e^{-ik_n t} \right]}{2k_n \omega_n^2 (e^{2\omega_n h} + 1)} \tag{19}$$

The unknown constants D_n and E_n shown in Equation (18) could be determined by applying the initial conditions.

Consider that, initially in the wave channel, water is still and there are no disturbances at the free surface. The initial conditions can be written as

$$\Phi(x, z, t) = 0, \quad t = 0 \tag{20}$$

$$\frac{\partial \Phi(x, z, t)}{\partial t} \Big|_{z=0} = 0, \quad t = 0 \tag{21}$$

Equations (20) and (21) should be rewritten according to the Fourier cosine transform, Equation (9), and provide two equations solving for the two constants. Thus, we obtained undetermined constants, shown in Equation (18):

$$D_n = \frac{1}{2i\omega_n^2 k_n (e^{2\omega_n h} + 1)} \left[\int \ddot{\xi} \cdot e^{-ik_n t} dt \Big|_{t=0} - ik_n \dot{\xi}(0) - \ddot{\xi}(0) \right] \tag{22}$$

$$E_n = \frac{1}{2i\omega_n^2 k_n (e^{2\omega_n h} + 1)} \left[- \int \ddot{\xi} \cdot e^{ik_n t} dt \Big|_{t=0} - ik_n \dot{\xi}(0) + \ddot{\xi}(0) \right] \tag{23}$$

So far, the potential function $\phi_n(z, t)$ is completely determined. Similar to obtaining $\phi_n(z, t)$, we also obtained $\phi_0(z, t)$ as

$$\phi_0(z, t) = -\dot{\xi} \left(\frac{z^2}{2} + hz \right) + gh \left(\int \ddot{\xi}(t) dt + \int \ddot{\xi}(t) dt \Big|_{t=0} - \dot{\xi}(0) \cdot t \right) \tag{24}$$

The initial boundary value problem described by Equations (2)–(6), (20), and (21) was solved.

Thus, the initial boundary value problem was solved. The wave potential function could be expressed explicitly as

$$\begin{aligned} \Phi(x, z, t) = & \frac{1}{\ell} \left[-\dot{\xi} \left(\frac{z^2}{2} + hz \right) + gh \left(\int \ddot{\xi}(t) dt + \int \ddot{\xi}(t) dt \Big|_{t=0} - \dot{\xi}(0) \cdot t \right) \right] \\ & + \frac{2}{\ell} \sum_1^\infty \left\{ \frac{ik_n (e^{2\omega_n h} e^{\omega_n z} + e^{-\omega_n z})}{2\omega_n^2 (e^{2\omega_n h} + 1)} \cdot \left[- \left(\int \ddot{\xi} \cdot e^{-ik_n t} dt - \int \ddot{\xi} \cdot e^{-ik_n t} dt \Big|_{t=0} \right) \cdot e^{ik_n t} \right. \right. \\ & \left. \left. + \left(\int \ddot{\xi} \cdot e^{ik_n t} dt - \int \ddot{\xi} \cdot e^{ik_n t} dt \Big|_{t=0} \right) \cdot e^{-ik_n t} + \frac{2i\dot{\xi}}{k_n} \right] + \frac{\dot{\xi}}{\omega_n^2} \right\} \cos(\omega_n x) \end{aligned} \tag{25}$$

For a piston type wavemaker, the displacement function of the wavemaker can be expressed as

$$\zeta(t) = -\frac{s_0}{2}e^{-i\omega t} \tag{26}$$

where s_0 is the stroke of the wavemaker motion, $\omega = 2\pi/T$, and T is the period of the wavemaker motion. Following the general analytical solution, Equation (25), the associated potential function for the generated wave can be written as

$$\begin{aligned} \Phi(x, z, t) = & \frac{-s_0}{2\omega\ell} \left[i\omega^2 z \left(\frac{z}{2} + h \right) e^{-i\omega t} + gh \left[i \left(e^{-i\omega t} - 1 \right) - \omega t \right] \right] \\ & + \frac{i\omega s_0}{\ell} \sum_1^\infty \left\{ \begin{aligned} & \frac{k_n \left(e^{2\omega_n h} e^{\omega_n z} + e^{-\omega_n z} \right)}{\omega_n^2 \left(e^{2\omega_n h} + 1 \right)} \cdot \left[\frac{-e^{ik_n t}}{2(\omega + k_n)} + \frac{e^{-ik_n t}}{2(\omega - k_n)} - \frac{k_n e^{-i\omega t}}{(\omega^2 - k_n^2)} \right] \\ & + \frac{e^{-i\omega t}}{\omega_n^2} \left[1 - \frac{\left(e^{2\omega_n h} e^{\omega_n z} + e^{-\omega_n z} \right)}{\left(e^{2\omega_n h} + 1 \right)} \right] \end{aligned} \right\} \cos(\omega_n x) \end{aligned} \tag{27}$$

The associated free surface elevation can be calculated from Equation (27) by using the Bernoulli’s equation and can be expressed as

$$\begin{aligned} \eta(x, t) = & \frac{s_0 h}{2\ell} \left(1 - e^{-i\omega t} \right) \\ & + \frac{\omega s_0}{g\ell} \sum_{n=1}^\infty \left\{ \frac{k_n^2}{\omega_n^2} \left[\frac{e^{ik_n t}}{2(\omega + k_n)} + \frac{e^{-ik_n t}}{2(\omega - k_n)} - \frac{\omega}{(\omega^2 - k_n^2)} e^{-i\omega t} \right] \right\} \cos(\omega_n x) \end{aligned} \tag{28}$$

Note that, for the piston type wavemaker problem, an analytical transient solution was presented by Lee [15] using a different solution methodology. In solving the initial and boundary-value problems, the Laplace transform was used to transform the time function, then solved the corresponding spatial functions, along with the boundary conditions and the final inverse Laplace transform to obtain the analytical solution. While we tried to utilize Lee [15]’s approach to solve other wavemaker problems, we found that the inverse Laplace transform may not be able to work; therefore, we devised new and different solution methods to solve the problem. After we obtained the present analytical solution, we thought that there could be only one solution for the same initial and boundary-value problem, and we proceeded to give proof.

We show that the real part expression of the free surface elevation, Equation (28), in the present solution can be mathematically manipulated to show be identical with Equation, (18), shown in Lee [15].

The exponential function shown in Equation (28) can be expressed by

$$e^{ir} = \cos r + i \sin r \tag{29}$$

With the substitution of Equation (29) into Equation (28), we obtain

$$\begin{aligned} \eta(x, t) = & \frac{hs_0}{2\ell} \{ 1 - \cos(\omega t) + i \sin(\omega t) \} \\ & + \frac{2}{g\ell} \sum_{n=1}^\infty \left\{ \frac{\omega s_0}{2\omega_n^2} \left[\frac{k_n^2}{2(\omega + k_n)} [\cos(k_n t) + i \sin(k_n t)] + \frac{k_n^2}{2(\omega - k_n)} [\cos(k_n t) - i \sin(k_n t)] \right] \right. \\ & \left. - \frac{\omega k_n^2}{(\omega^2 - k_n^2)} [\cos(\omega t) - i \sin(\omega t)] \right\} \cos(\omega_n x) \end{aligned} \tag{30}$$

The real part of the free surface elevation, Equation (30), could be expressed as

$$\begin{aligned} \text{Re}[\eta(x, t)] &= \frac{s_0 h}{2\ell} [1 - \cos \omega t] \\ &+ \frac{\omega^2 s_0}{g\ell} \sum_{n=1}^{\infty} \frac{k_n^2}{\omega_n^2 (\omega^2 - k_n^2)} [\cos(k_n t) - \cos(\omega t)] \cos(\omega_n x) \end{aligned} \tag{31}$$

Next, we adopted the variable definitions used in Lee [15]. A cross reference of symbols between Lee [15] and present formulation is shown in Table 1.

Table 1. Cross Reference of symbols between Lee [15] and present formulation.

present theory	ℓ	$s_0/2$	ω	z	h	k_n	ω_n
Lee [15]	L	a	σ	y	h	k_n	ω_n

After some mathematical rearrangements, Equation (31) can be rewritten as

$$\begin{aligned} \eta(x, t) &= \frac{ha}{L} \{1 - \cos(\sigma t)\} \\ &+ \frac{2a\sigma^2}{gL} \sum_{n=1}^{\infty} \frac{1}{\omega_n^2} \left\{ \frac{1}{(k_n^2 - \sigma^2)} [\sigma^2 \cos(\sigma t) - k_n^2 \cos(k_n t)] + \cos(\sigma t) \right\} \cos(\sigma_n x) \end{aligned} \tag{32}$$

Equation (32) is precisely identical to the expression shown in Lee [15], which confirms the present analytical solution. We like to emphasize that, although the free surface elevation obtained in this study, Equation (28), was proved identical with the expression in Lee [15], the derivation to obtain the analytical solution is entirely different from Lee [15]. Furthermore, without having the inverse Laplace transform, the present analytical method could be applied to solve other problems more easily.

In the next section, convergence of the series expression shown in the present analytical solution is be discussed first. Then, the wave forms generated by the transient solution are shown to match the steady wave theory in the fully developed state. Additionally, the transient wave length is compared with the steady wave length to show transient characteristics of wave length variation. In particular, the first wave length in front of the wavemaker is shown to include both propagating and evanescent waves. Secondly, the present analytical solution is compared with numerical solution and experimental results to validate wave form distribution along the wave flume. Finally, transient characteristics of the generated leading waves are investigated.

3. Results and Discussion

The present analytical solution for the wavemaker problem contains the cosine series expression. To calculate the generated free surface elevation, a finite number of terms should be determined in the computation. A result of convergence test is shown in Figure 2. The vertical axis is the dimensionless surface elevation, the subscript N indicates the number of terms used of the series expression, and A is the amplitude of the generated steady wave form. The conditions used in the calculation were $h = 0.2$ m, $s_0 = 0.035$ m, $T = 0.98$ s. The relative water depth, $Kh = 1.06$, falls in the range of intermediate water depth. The generated steady fully developed wave height and wave length are 3.67 m and 1.18 m, respectively, as calculated from the steady wave theory [27]. Figure 2 shows convergence of the series solution; where an error criterion 0.1% is adopted, the number of terms $N = 178$ should be used, as indicated by the dash vertical line in the figure. The relative error criterion is defined as

$$\text{error}\% = \left| \frac{(\eta_N - \eta_{N-1})}{\eta_{N-1}} \right| \cdot 100\% \tag{33}$$

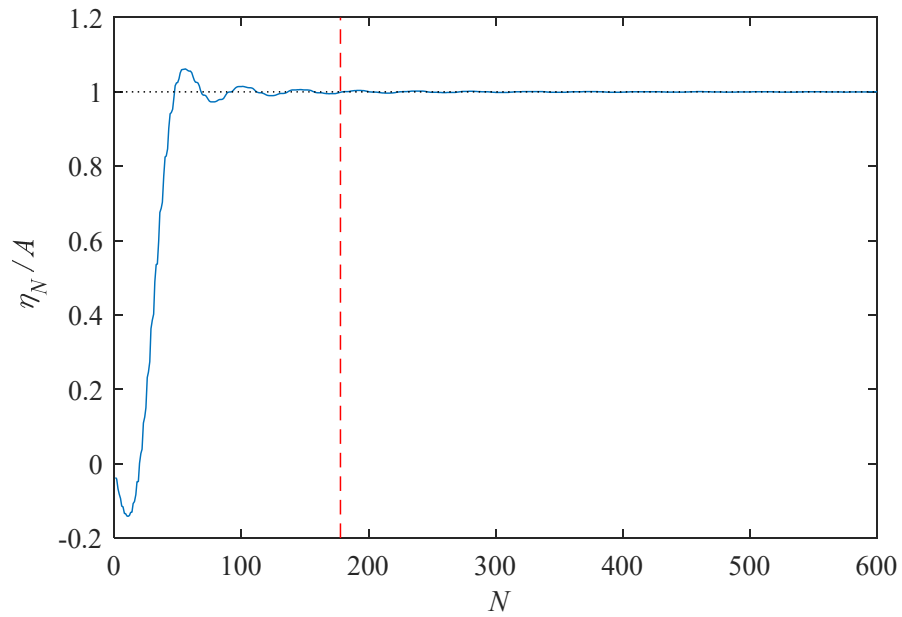


Figure 2. Dimensionless surface elevation versus number of terms of the cosine series.

Time evolution of the generated surface waves at a fixed location of the wave channel is shown in Figure 3, where $h = 0.3$ m, $s_0 = 0.052$ m, $T = 0.82$ s, and $kh = 1.88$. The observatory location is one wave length away from the wavemaker. The gain function, $\eta/(s_0/2)$, calculated from the steady wavemaker theory, is also plotted to show the envelopes of the developed wave amplitudes with time as the upper and lower dash lines. Figure 3 shows that the fully developed wave heights follow the envelopes of the steady state solution. Furthermore, the wave forms take four waves to reach the fully developed state, and the developing rates of the wave form are illustrated.

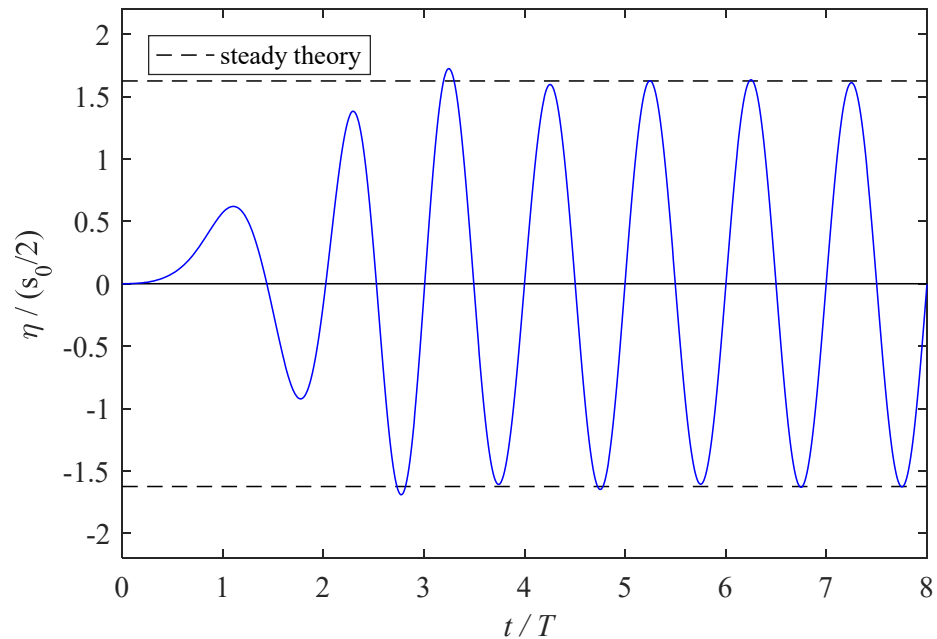


Figure 3. Surface evolution with time at a fixed location. ($T = 0.82$ s, $kh = 1.88$).

The distribution of surface wave along the channel at a fixed time after waves are generated is plotted in Figure 4. The horizontal axis is a dimensionless distance away from the wavemaker, and L_0 is the steady wave length. The vertical axis is the dimensionless surface elevation. The conditions used are $h = 0.3$ m, $s_0 = 0.037$ m, and $T = 1.08$ s, and

15 wave periods are calculated. The steady wave form calculated using the steady solution is plotted in phase with the present theory for comparison. Figure 4 shows that the generated fifth wave almost has the same wave length as the steady result. The leading first wave has approximately 4.5 times the steady wave length, and the following wave lengths decrease gradually and reduce to the steady result.

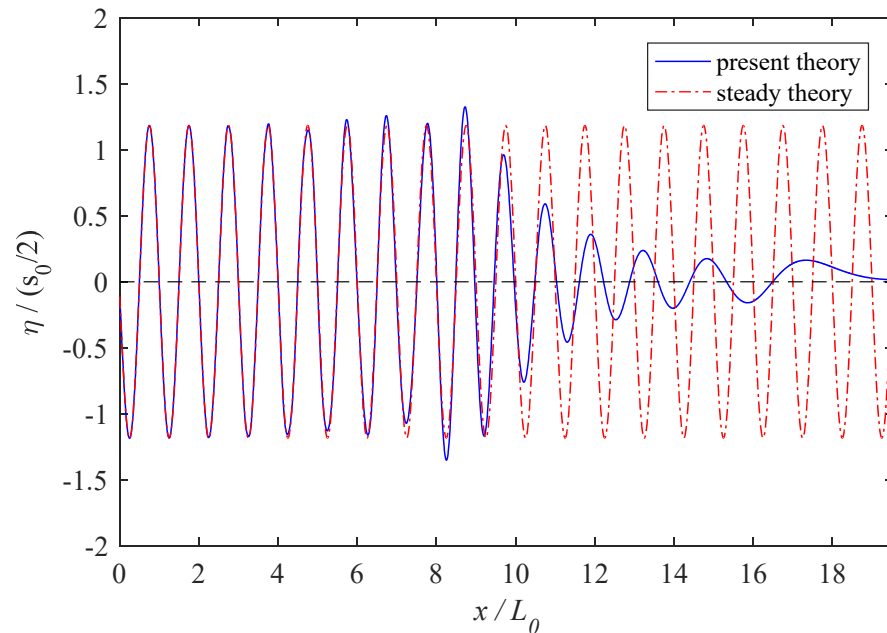


Figure 4. Wave elevations along the channel at $t = 15T$.

In the wavemaker theory, motions of the wavemaker generate propagating waves and accompanied evanescent waves that decay while moving away from the wavemaker. In front of the wavemaker, the fully developed wave form calculated by the present analytical solution, the steady theory, and the propagating waves are plotted in Figure 5. Figure 5 shows that after the waves are fully developed, the present time domain solution (line) precisely matches the wave length and amplitude as the steady theory (circle). On the other hand, the difference between steady wave form and the propagating wave form (red dash line) indicates the evanescent wave in front of the wavemaker.

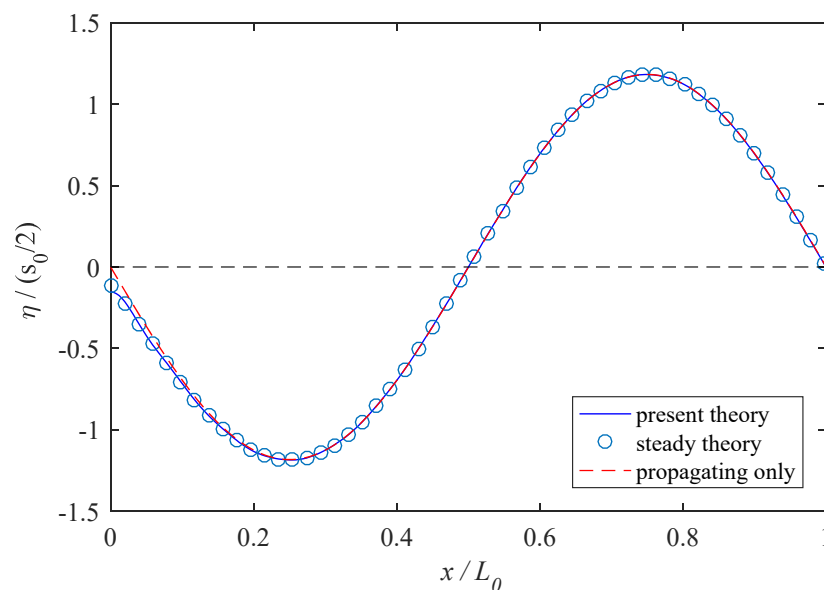


Figure 5. The first wave form in front of the wavemaker boundary.

The generated surface waves by the wavemaker at 8.0 s, calculated using Equation (31), was validated with the numerical boundary element solution, as shown in Figure 6. The result is cited from Figure 13 in Lee [15]. The conditions used were water depth 3 m, length of the channel 30 m, stroke, and period of the wavemaker at 1.0 m and 2.0 s, respectively. The comparisons of the unsteady wave profiles were in reasonable agreements. The present analytical solution and the numerical solution matched very well for the first wave length. For the rest of the wave forms, the numerical solutions had slightly higher wave peaks and shallower wave troughs, with maximum 5% differences. The present analytical solution was further used to simulate experimental results presented by Gao [29]. In the experiments, the water depth was 0.28 m and the stroke and period of the wavemaker motion were 0.02 m and 1 s, respectively. The length of the wave channel was 8.75 m. Variation of the free surface elevation with time at a location 0.55 m in front of the wavemaker was used for comparison. Calculated results using present analytical solution (line) and experimental results (discrete star) copied from Gao [29] are plotted in Figure 7. The comparison shows favorable agreements. Note that the wave amplitude calculated by using the steady wavemaker theory was 0.0125 m. At wave peaks, the two results match the steady theory; however, at wave troughs, the present analytical solution matches the steady theory, but the experimental results are shallower, and the differences are approximately 12%.

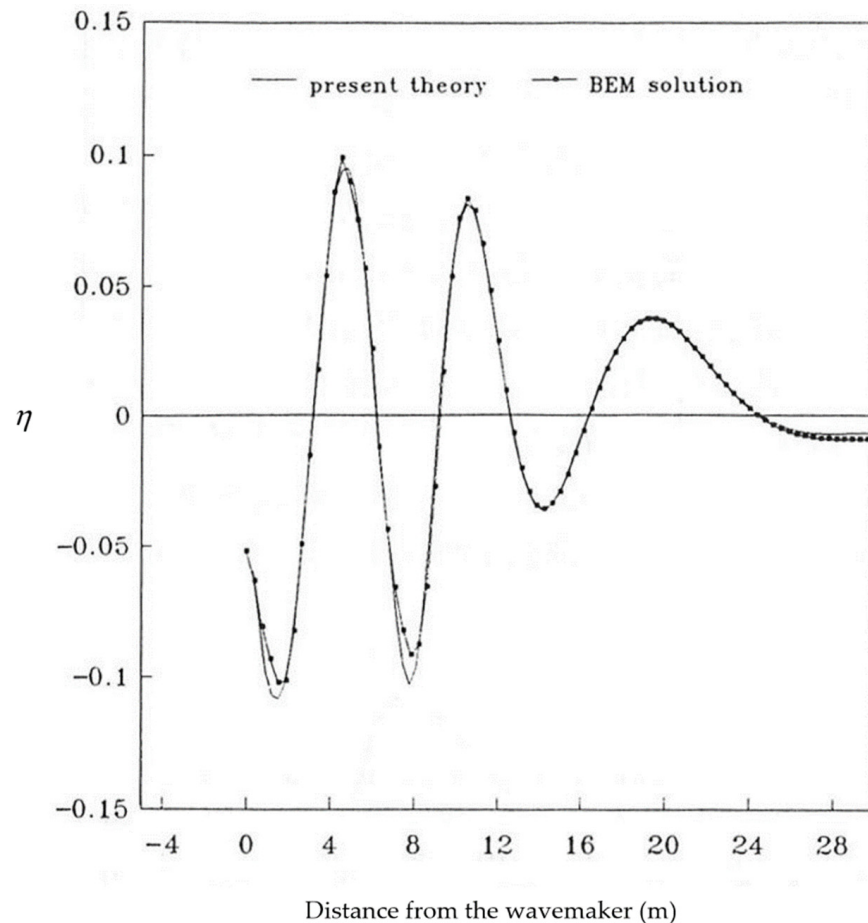


Figure 6. Comparison of free surface elevation between analytical solution and numerical solution (cited from Figure 13, Lee [15]).

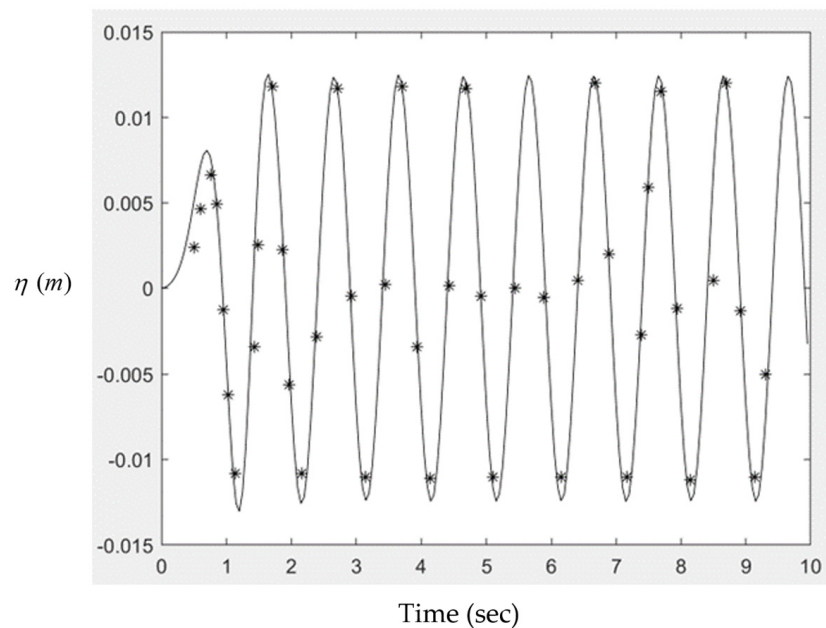


Figure 7. Comparison of free surface elevation between present solution (line) and experimental results (discrete star) [29].

The present analytical solution can be used to simulate transient development of waves generated by the wavemaker in a channel. Time variations of surface waves in front of the wavemaker along the wave channel at one-period time, two-periods, six-periods, and 10-periods of the wavemaker motion are shown in Figure 8. At time one-period, a developing wave form is induced, where a smaller wave peak is ahead of a lower trough propagating away from the wavemaker. At the two-period time, two wave forms are generated along the channel. A smaller wave is propagating ahead of a bigger wave, while waves are propagating away from the wavemaker. The wave forms are gradually developing, and it is expected that as more waves are continuously generated, the wave forms will reach fully developed conditions. At the six-period time, there are six unsteady waves in front of the wavemaker; among them there are four developed waves behind the two smaller leading waves. As for the 10-period time, there are four fully developed waves behind the four leading transient waves. We can notice that between fully developed waves and the leading waves, there is a highest wave. The simulated results indicated that there is a relatively bigger wave between developing waves and fully developed steady waves, which is about 15% bigger than the steady wave heights. As more time elapsed, there will be more fully developed waves generated following the leading waves.

Using the present analytical solution, we calculated the generated waves to investigate unsteady characteristics of the wave heights and wave lengths of the leading waves. The conditions used are water depth 0.35 m, the stroke of the wavemaker motion 0.019 m, and the wavemaker periods 1.14 s, 1.52 s, 1.95 s, and 2.56 s. Figure 9 shows variations of dimensionless wave height versus dimensionless time, where H_0 is the steady wave height and H_S is the wave height of the leading waves. Overall, the wave heights of the leading waves decrease as they propagate away from the wavemaker. For shorter waves, the wave heights decrease rapidly in the beginning five periods of time; on the other hand, for longer wave periods, the wave heights decrease rapidly in the beginning 15 periods of time. For 25 to 35 periods of time, the wave heights decrease and become gradual, showing a tendency of reaching constants. The shorter waves reach 0.1 and the longer waves reach 0.2. Figure 10 shows variations of dimensionless wave lengths of the leading waves versus dimensionless time, where L_0 is the steady wave length and L_S is the wave length of the leading waves. The wave length of the leading wave is defined as the distance starting from the raised water front to the first following zero-up crossing. In general, the wave lengths

of the leading waves increase with time as they propagate away from the wavemaker. The calculated results indicate that for longer waves, tendency of wave length increase will reach 3.5; on the other hand, for shorter waves, the tendency will reach 7.

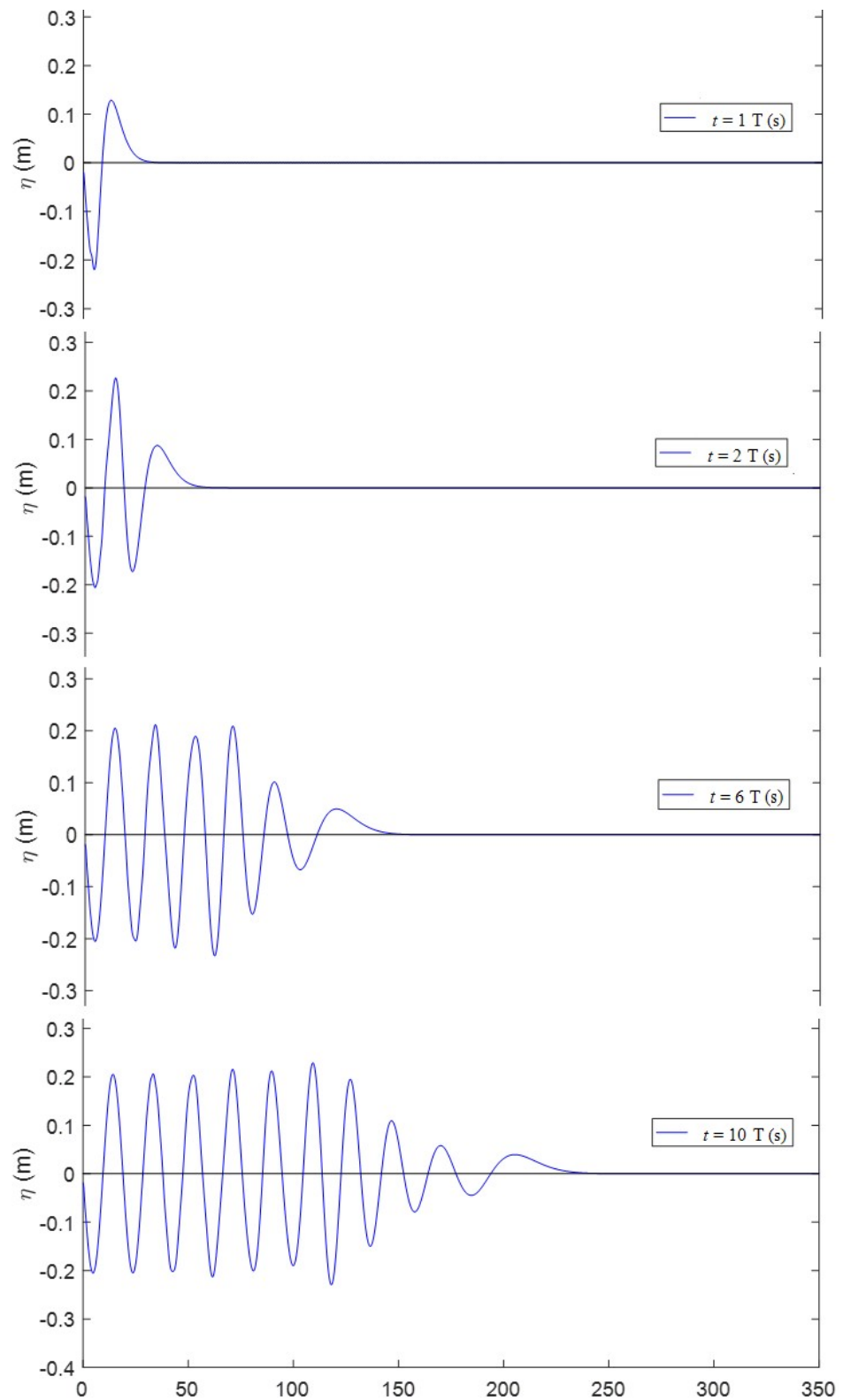


Figure 8. Generated waves along the wave channel for one, two, six, and 10 periods.

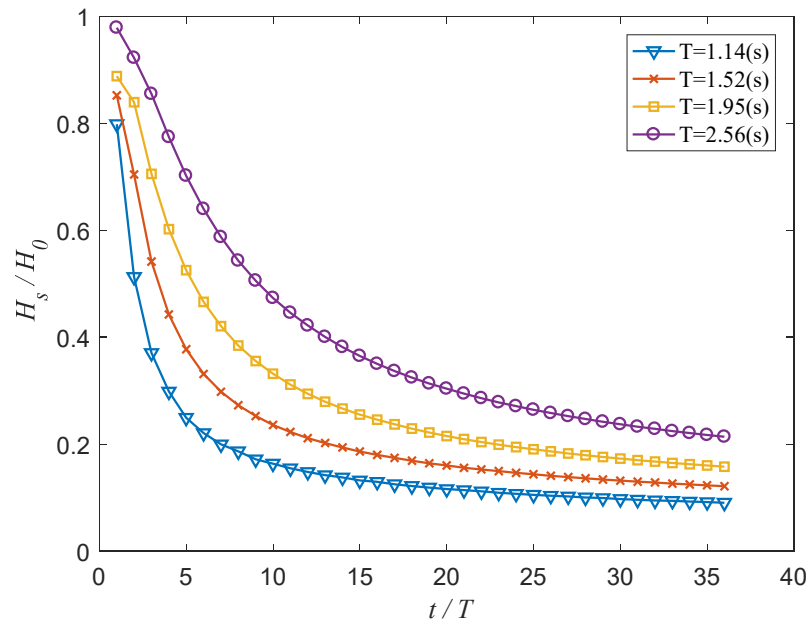


Figure 9. Variation of wave height versus time (period) of the leading wave.

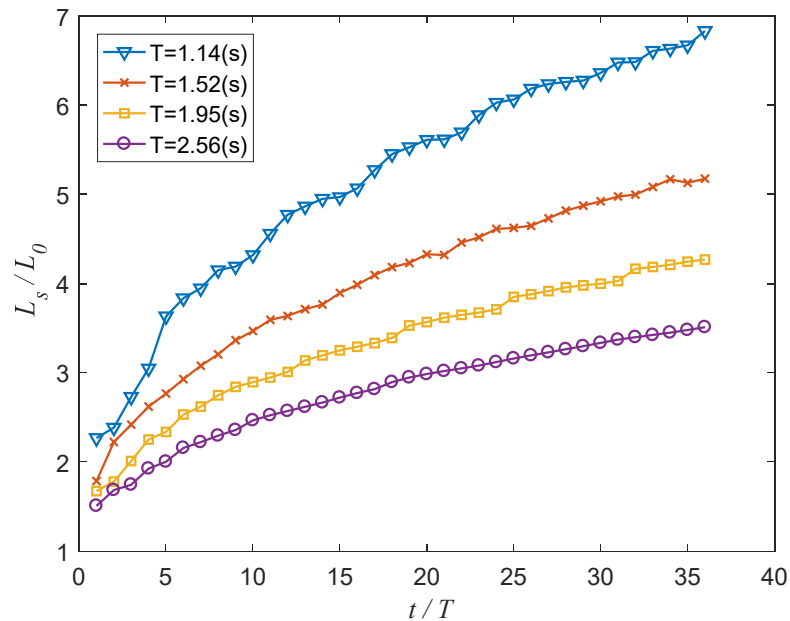


Figure 10. Variation of wave length versus time (period) of the leading wave.

4. Conclusions

A new analytical solution is presented for the transient wavemaker problem in a wave channel. The linear potential wave theory was applied, and an initial boundary-value problem was established to solve the problem. The solution methodology was developed from previous methods in the literature and can provide an easier solution method to obtain the solution analytically. In the present solution methodology, the spatial functions were obtained by solving the nonhomogeneous second-order differential equations given by the Fourier cosine transform, whereas the time-dependent function was obtained by using the free surface boundary condition. Our analytical solution forms can be manipulated mathematically and shown to be identical to the previous solution obtained using different solution methodology. However, the entire derivations are different and more straightforward and efficient. The fully developed wave form generated from transient solution compared very well with the steady state wavemaker theory. The steady wave

form shows the propagation waves and evanescent waves in front of the wavemaker. The transient waveforms compare favorably well with the numerical solution with a 5% difference and show comparisons with experimental results with a 12% difference. Unsteady characteristics of wave heights and wave lengths of the leading waves are presented. We can apply the present transient wavemaker solution to simulate the evolutions of surface waves generated in the wave channel.

Author Contributions: Conceptualization, J.-F.L. and C.-T.C.; methodology, J.-F.L., C.-T.C., P.-S.H. and K.-T.L.; validation, K.-T.L. and P.-S.H.; writing—original draft preparation, J.-F.L. and C.-T.C.; writing—review and editing, J.-F.L. and C.-T.C.; project administration, J.-F.L. and C.-T.C.; funding acquisition, C.-T.C. and J.-F.L. All authors have read and agreed to the published version of the manuscript.

Funding: This research was funded by Sanming University, under grant number 22YG01, and by the Ministry of Science and Technology, Taiwan, grant number MOST-108-2221-E-006-084.

Institutional Review Board Statement: Not applicable.

Informed Consent Statement: Not applicable.

Data Availability Statement: Not applicable.

Acknowledgments: Financial support from Sanming University under Grant Number 22YG01 and the Ministry of Science and Technology, Taiwan, under Grant Number MOST-108-2221-E-006-084, are gratefully acknowledged.

Conflicts of Interest: The authors declare no conflict of interest.

References

1. Khait, A.; Shemer, L. Nonlinear wave generation by a wavemaker in deep to intermediate water depth. *Ocean Eng.* **2019**, *182*, 222–234. [[CrossRef](#)]
2. He, M.; Khayyer, A.; Gao, X.; Xu, W.; Liu, B. Theoretical method for generating solitary waves using plunger-type wavemakers and its Smoothed Particle Hydrodynamics validation. *Appl. Ocean Res.* **2021**, *106*, 102414. [[CrossRef](#)]
3. Sun, B.; Li, C.; Yang, S.; Zhang, H. A simplified method and numerical simulation for wedge-shaped plunger wavemaker. *Ocean Eng.* **2021**, *241*, 110023. [[CrossRef](#)]
4. Stoker, J.J. *Water Waves*; Interscience Publishers Inc.: New York, NY, USA, 1957.
5. Jang, T.S.; Sung, H.G. New nonlinear theory for a piston-type wavemaker: The classical Boussinesq equations. *Appl. Math. Model.* **2020**, *91*, 43–57. [[CrossRef](#)]
6. Wei, G.; Kirby, J.T. Time-Dependent Numerical Code for Extended Boussinesq Equations. *J. Waterw. Port Coast. Ocean Eng.* **1995**, *121*, 251–261. [[CrossRef](#)]
7. De Padova, D.; Mossa, M.; Sibilla, S. Characteristics of nonbuoyant jets in a wave environment investigated numerically by SPH. *Environ. Fluid Mech.* **2020**, *20*, 189–202. [[CrossRef](#)]
8. Ozbulut, M.; Ramezanzadeh, S.; Yildiz, M.; Goren, O. Modelling of wave generation in a numerical tank by SPH method. *J. Ocean Eng. Mar. Energy* **2020**, *6*, 121–136. [[CrossRef](#)]
9. Gholamipoor, M.; Ghiasi, M. Simulation of fully nonlinear water wave propagation over the flat bottom and uneven bottom by meshless numerical wave tank. *Ing. Arch.* **2021**, *91*, 4329–4341. [[CrossRef](#)]
10. Vivanco, I.; Cartwright, B.; Araujo, A.L.; Gordillo, L.; Marin, J. Generation of Gravity Waves by Pedal-Wavemakers. *Fluids* **2021**, *6*, 222. [[CrossRef](#)]
11. Jacobsen, N.G.; Fuhrman, D.R.; Fredsøe, J. A wave generation toolbox for the open-source CFD library: OpenFoam[®]. *Int. J. Numer. Methods Fluids* **2012**, *70*, 1073–1088. [[CrossRef](#)]
12. Higuera, P.; Lara, J.L.; Losada, I.J. Realistic wave generation and active wave absorption for Navier–Stokes models. *Coast. Eng.* **2012**, *71*, 102–118. [[CrossRef](#)]
13. Martínez-Ferrer, P.J.; Qian, L.; Ma, Z.; Causon, D.M.; Mingham, C.G. Improved numerical wave generation for modelling ocean and coastal engineering problems. *Ocean Eng.* **2018**, *152*, 257–272. [[CrossRef](#)]
14. Lee, J.-F.; Kuo, J.-R.; Lee, C.-P. The Transient wavemaker theory. *J. Hydraul. Res.* **1989**, *27*, 651–663. [[CrossRef](#)]
15. Lee, J.F. Theoretical analysis of wave generation by piston-type wavemaker. *J. Harb. Technol.* **1991**, *6*, 23–40. (In Chinese)
16. Joo, S.W.; Schultz, W.W.; Messiter, A.F. An analysis of the initial-value wavemaker problem. *J. Fluid Mech.* **1990**, *214*, 161–183. [[CrossRef](#)]
17. Chang, H.-K.; Lin, S.-C. An Analytical Linear Solution of Transient Waves Generated by a Piston-Type Wave-Maker in a Finite Flume. *J. Coast. Ocean Eng.* **2009**, *9*, 25–41. [[CrossRef](#)]

18. Lin, S.-C.; Chang, H.-K. An Analytical Wave-Maker Theory for Irregular Waves in a Finite Channel. *J. Coast. Ocean Eng.* **2009**, *9*, 225–238. [[CrossRef](#)]
19. Berry, M.V. Minimal analytical model for undular tidal bore profile; quantum and Hawking effect analogies. *N. J. Phys.* **2018**, *20*, 053066. [[CrossRef](#)]
20. El, G.A.; Grimshaw, R.H.J.; Smith, N.F. Unsteady undular bores in fully nonlinear shallow-water theory. *Phys. Fluids* **2006**, *18*, 027104. [[CrossRef](#)]
21. Landrini, M.; Tyvand, P.A. Generation of water waves and bores by impulsive bottom flux. *J. Eng. Math.* **2001**, *39*, 131–170. [[CrossRef](#)]
22. Marchant, T.R. Undular bores and the initial-boundary value problem for the modified Korteweg-de Vries equation. *Wave Motion* **2008**, *45*, 540–555. [[CrossRef](#)]
23. Bestehorn, M.; Tyvand, P.A. Merging and colliding bores. *Phys. Fluids* **2009**, *21*, 042107. [[CrossRef](#)]
24. Ali, A.; Kalisch, H. A dispersive model for undular bores. *Anal. Math. Phys.* **2012**, *2*, 347–366. [[CrossRef](#)]
25. Chen, C.-T.; Lee, J.-F.; Chanson, H.; Lin, K.-T.; Lin, C.-J. A Time-Domain Analytic Solution of Flow-Induced Undular Bores. *J. Mar. Sci. Eng.* **2022**, *10*, 738. [[CrossRef](#)]
26. Tong, L.; Liu, P.L.-F. Transient wave-induced pore-water-pressure and soil responses in a shallow unsaturated poroelastic seabed. *J. Fluid Mech.* **2022**, *938*, A36. [[CrossRef](#)]
27. Dean, R.G.; Dalrymple, R.A. *Water Wave Mechanics for Engineers and Scientists*; World Scientific Publishing Co. Ltd.: Singapore, 1991. [[CrossRef](#)]
28. Kreyszig, E. *Advanced Engineering Mathematics*, 10th ed.; John Wiley & Sons Inc.: Hoboken, NJ, USA, 2011; pp. 154–196; ISBN 9780470458365.
29. Gao, F. An Efficient Finite Element Technique for Free Surface Flo. Ph.D. Thesis, University of Brighton, Brighton, UK, 2003.